Journal of
Computational and Theoretical Nanoscience
Volume 5, Issue 4, Pages 639-646, 2008
DOI:10.1166/jctn.2008.030

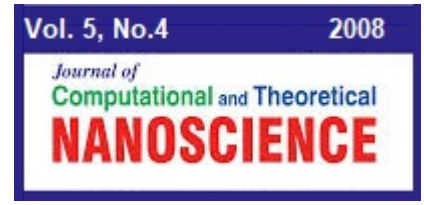

Volumetric Dependence of Interatomic Distance in Dense Nanosystems: A Theoretical and Molecular Dynamics Study

Pirooz Mohazzabi[1, 2, *] and **G.Ali Mansoori**[3]

[1] *Department of Physics, University of Wisconsin-Parkside, Kenosha, Wisconsin 53141, USA*
[2] *Departments of Bioengineering, University of Illinois at Chicago, Chicago, Illinois 60607, USA*
[3] *Departments of Bioengineering and Chemical Engineering, University of Illinois at Chicago, Chicago, Illinois 60607, USA*

ABSTRACT:

Theoretical and molecular dynamics simulations of small dense argon systems suggest functional forms for the dependence of internal energy and internal pressure on volume that are quite different from those in macroscopic systems. The results strongly suggest that the proportionality between volume of a system and the mean nearest-neighbor distance between its particles breaks down in nanosystems. The qualitative behaviors of the internal energy and internal pressure, however, are independent of the system size and are the same in both large and small systems.

Keywords: Nanosystems, Internal Energy, Internal P ressure, Volume Dependence, Nearest-Neighbor Distance.

RESEARCH ARTICLE

1. BACKGROUND

The laws of thermodynamics for small systems are in principle similar to those for macroscopic systems. However, for small systems the validity of the relationships among various thermodynamic properties that normally apply to macroscopic systems is an open question. Consequently, in many respects small systems deviate from macroscopic ones. These effects, which are predominantly due to limited number of particles and large surface-to-volume ratio in small systems have been discussed elsewhere, beginning with Hill[1] who introduced the concept of thermodynamics of small systems in 1963.[2–6]

Recently we studied the question of extensivity and intensivity in nanosystems[7] using molecular dynamics simulations. We investigated the extensivity of internal energy and entropy as well as the intensivity of temperature and pressure in these small systems. We found that, in contrast to macroscopic systems and in agreement with their theoretical predictions, in many small systems internal energy is nonextensive and pressure is nonintensive.

Thermodynamics and statistical mechanics of macroscopic systems are well understood and the connection between their thermodynamic properties and molecular characteristics are derived. The basic principles of thermodynamics and statistical mechanics for small systems have been recently formulated.[8] For macroscopic systems, consisting of very large number of particles in equilibrium, these thermodynamic relations are already well established.[9–11] On the other hand, the relationships predicted by the thermodynamics of small systems have not been fully tested by statistical models.

Small systems of interest in nanotechnology generally consist of condensed matter of various kinds, soft or hard, organic or inorganic, and/or biological ingredients. An understanding of the nature of interactions between the individual atoms and molecules in such systems as well as their statistical mechanics are essential to nanotechnology. Furthermore it is well-known that, contrary to macroscopic systems, the behavior of matter confined in nano-containers (inside a nanotube, etc.) is a function of the environmental geometry, size, and wall effects that are surrounding it.

Motivated by these concepts, we decided to investigate the functional forms of the dependence of internal energy and internal pressure on volume in small systems and to compare them with those in macroscopic systems. This investigation is important as it can provide clues and shed light on the relationship between the volume of a small system and the mean nearest-neighbor distance between its particles, a proportionality that is normally assumed in large systems.

2. THEORETICAL CONSIDERATIONS

We consider a three-dimensional system consisting of N identical particles interacting pairwise according to the

(*). Corresponding author, email: *mohazzab@uwp.edu*

Lennard-Jones (6-12) potential energy function,

$$\phi_{ij} = 4\epsilon\left[\left(\frac{\sigma}{r_{ij}}\right)^{12} - \left(\frac{\sigma}{r_{ij}}\right)^{6}\right] \tag{1}$$

where the constants σ and ϵ are the diameter at zero potential and the potential depth, respectively. The internal energy of this system is given by

$$U = \frac{1}{2}m\sum_{i=1}^{N} v_i^2 + 4\epsilon\frac{N}{2}\sum_{j(\neq i)=1}^{N}\left[\left(\frac{\sigma}{r_{ij}}\right)^{12} - \left(\frac{\sigma}{r_{ij}}\right)^{6}\right] \tag{2}$$

in which the factor 1/2 in the potential energy term is introduced to avoid counting each term twice. The total kinetic energy term can be written in terms of the ensemble average $\langle v^2\rangle$. Furthermore, we may write the distance between particle i and particle j in terms of the system's mean nearest-neighbor distance $\bar{R}$,

$$r_{ij} = p_{ij}\bar{R} \tag{3}$$

where p_{ij} is a positive dimensionless quantity. Thus, Eq. (2) reduces to

$$U = \frac{1}{2}Nm\langle v^2\rangle + 2N\epsilon\sum_{j(\neq i)=1}^{N}\left[p_{ij}^{-12}\left(\frac{\sigma}{\bar{R}}\right)^{12} - p_{ij}^{-6}\left(\frac{\sigma}{\bar{R}}\right)^{6}\right] \tag{4}$$

and further to

$$U = \frac{1}{2}Nm\langle v^2\rangle + 2N\epsilon\left[s_{12}\left(\frac{\sigma}{\bar{R}}\right)^{12} - s_6\left(\frac{\sigma}{\bar{R}}\right)^{6}\right] \tag{5}$$

where the positive dimensionless structure sums s_{12} and s_6 are defined by

$$s_{12} = \sum_{j(\neq i)=1}^{N} p_{ij}^{-12} \quad \text{and} \quad s_6 = \sum_{j(\neq i)=1}^{N} p_{ij}^{-6} \tag{6}$$

According the equipartition theorem,[25] the nonrelativistic ensemble average of the translational kinetic energy of the particles is equal to $(3/2)kT$. Therefore, Eq. (5) becomes

$$U = \frac{3}{2}NkT + 2N\epsilon\left[s_{12}\left(\frac{\sigma}{\bar{R}}\right)^{12} - s_6\left(\frac{\sigma}{\bar{R}}\right)^{6}\right] \tag{7}$$

We now introduce two key assumptions in our calculations. The first, which is often used in the literature, but to the best of our knowledge has never been proven, is that the volume of a thermodynamic system with a fixed number of particles is proportional to the cube of the mean nearest-neighbor distance between its particles,[13]

$$\frac{V}{N} = c\bar{R}^3 \tag{8}$$

where c is a positive dimensionless constant which is inversely proportional to the packing factor of the system. Although this assumption seems reasonable for macroscopic systems, its validity in small systems where the concept of mean nearest-neighbor distance is not clearly defined, is still an open question.

The second assumption is that for a fixed number of particles, as the volume of the system (and hence density) changes, the structure sums s_{12} and s_6 remain constant even though the individual terms in their defining Eqs. (6) may change. Under these assumptions Eq. (7) reduces to

$$U = \frac{3}{2}NkT + 2N\epsilon\left[\gamma_4\left(\frac{N\sigma^3}{V}\right)^4 - \gamma_2\left(\frac{N\sigma^3}{V}\right)^2\right] \tag{9}$$

where the positive dimensionless constants γ_4 and γ_2 are defined by

$$\gamma_4 = s_{12}c^4 \quad \text{and} \quad \gamma_2 = s_6c^2 \tag{10}$$

For a simple macroscopic system with a constant number of molecules, the differential of the internal energy can be written in the classical form of the second law of thermodynamics as[14]

$$dU = TdS - PdV \tag{11}$$

Dividing both sides of this equation by dV and imposing the condition of constant temperature, we find

$$\left(\frac{\partial U}{\partial V}\right)_T = T\left(\frac{\partial S}{\partial V}\right)_T - P \tag{12}$$

Then using the Maxwell relation

$$\left(\frac{\partial S}{\partial V}\right)_T = \left(\frac{\partial P}{\partial T}\right)_V \tag{13}$$

we obtain

$$\left(\frac{\partial U}{\partial V}\right)_T = T\left(\frac{\partial P}{\partial T}\right)_V - P \tag{14}$$

The left hand side of Eq. (14) has the dimensions of pressure and is known as the *internal pressure* of the system,

$$P_{\text{int}} = \left(\frac{\partial U}{\partial V}\right)_T \tag{15}$$

However, we emphasize that internal pressure is not the true pressure of the system; the latter being the volume rate of change of the internal energy evaluated at constant entropy,

$$P = \left(\frac{\partial U}{\partial V}\right)_S \tag{16}$$

Equation (14) is of exceptional importance in thermodynamics.[15] For an ideal gas the internal pressure vanishes. This can be verified independently by evaluating either the left-hand side or the right-hand side of Eq. (14). The equation is, therefore, particularly useful in exploring the properties of imperfect gases. More specifically, because the right-hand side of Eq. (14) involves the equation of state only, it can provide information about the internal energy of an imperfect gas from its equation of state.

Experimentally it is found that isotherms of the internal energy of a number of dense fluids as a function

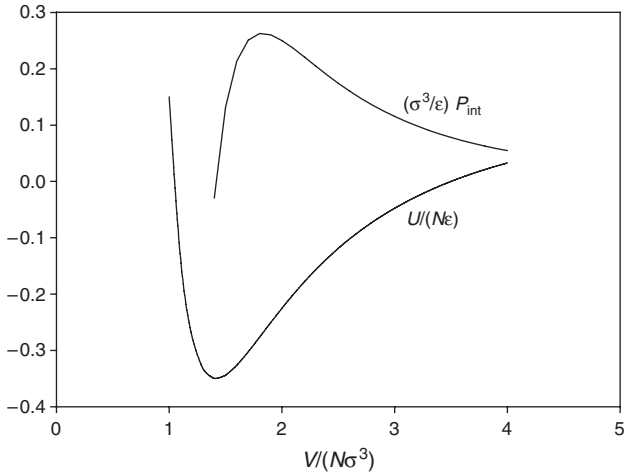

Fig. 1. Dimensionless plots of internal energy and internal pressure versus volume at constant temperature and particle number for a system obeying Lennard-Jones (6-12) potential energy function.

of molar volume show a minimum and those of their internal pressure versus molar volume show a maximum.[13] If one assumes that the two assumptions leading to Eq. (9) are valid, then these apparent anomalies can easily be understood based on a simple explanation. A dimensionless plot of Eq. (9) at constant temperature is represented in Figure 1. This function has a minimum at

$$\frac{V}{N\sigma^3} = \left(\frac{2\gamma_4}{\gamma_2}\right)^{1/2} \tag{17}$$

and a point of inflection at

$$\frac{V}{N\sigma^3} = \left(\frac{10\gamma_4}{3\gamma_2}\right)^{1/2} \tag{18}$$

Consequently, a plot of the internal pressure versus volume

$$P_{\text{int}} = \left(\frac{\partial U}{\partial V}\right)_T = \frac{4\epsilon}{\sigma^3}\left[-2\gamma_4\left(\frac{N\sigma^3}{V}\right)^5 + \gamma_2\left(\frac{N\sigma^3}{V}\right)^3\right] \tag{19}$$

has a zero at the minimum of U, and a maximum at the inflection point of U, as shown in Figure 1.

3. EXPERIMENTAL RESULTS AND MOLECULAR DYNAMICS SIMULATIONS

3.1. Macroscopic Systems

Because argon is a system for which interactions between its atoms are well described by the Lennard-Jones (6-12) potential energy function, we have based the bulk of our investigation on this system. Recently, Goharshadi et al. reported a comparison of the molecular dynamics results of 5000 particles and the experimental data for internal energy of argon as a function of molar volume at 180 K, which are in good agreement.[16]

If the two assumptions leading to Eq. (9) are conceivable, a function of the form

$$U = c_{-4}V^{-4} + c_{-2}V^{-2} + c_0 \tag{20}$$

with c_{-4}, c_{-2}, and c_0 constants should produce a least-squares fit to the experimental data that would be in good agreement with those reported by Goharshadi et al. Furthermore, the constant c_0 obtained from such a fit should agree with the kinetic energy per mole of the system, $(3/2)RT$, which has a value of 2245 J at 180 K.

A least-squares fit of the function in Eq. (20) to the experimental data for argon at 180 K gives

$$\begin{bmatrix} c_{-4} = 1.41956 \times 10^9\ \text{J}\cdot(10^{-2}\,\text{m})^{12} \\ c_{-2} = -4.87683 \times 10^6\ \text{J}\cdot(10^{-2}\,\text{m})^{6} \\ c_0 = 977.072\ \text{J} \end{bmatrix} \tag{21}$$

where, for the sake of convenience, we have used a unit of 10^{-2} m for length so that the unit of volume in Eq. (20) becomes 10^{-6} m^3. We note that the constant c_{-2} is negative, as it should be, according to Eq. (9). The value of the constant c_0, however, does not agree with the kinetic energy of the system. We will explain the reason for this discrepancy in a later section. Nevertheless, as can be seen in Figure 2, the agreement between the best fit and the data reported by Goharshadi et al. is striking.

Goharshadi et al. also plotted the internal pressure of the macroscopic argon system as a function of molar volume (plots similar to that in Fig. 1) at four different temperatures. These plots reveal two interesting features. First, the position of the maximum of internal pressure shifts to the right (larger volumes) as the temperature of the system

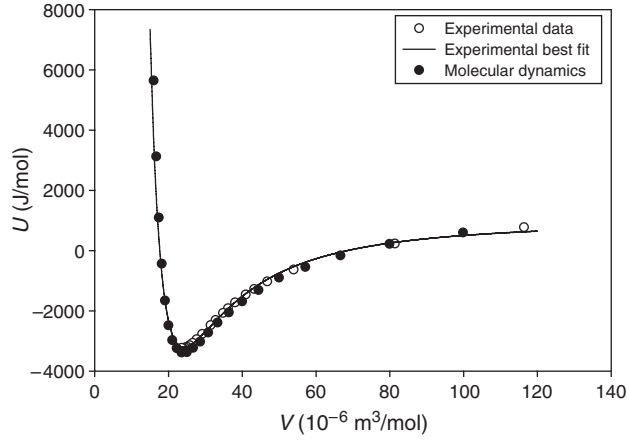

Fig. 2. Comparison between experimental data, their least-square fit, and molecular dynamics simulation of the internal energy of a macroscopic argon system at 180 K. The experimental data and the molecular dynamics simulations are from Goharshadi et al. Reprinted with permission from [16], E. K. Goharshadi et al., *Chem. Phys.* 331, 332 (**2007**). © 2007.

increases. This can be explained as follows: according to Eq. (20) the internal energy has a minimum at

$$V_{\min} = \left(-\frac{2c_{-4}}{c_{-2}}\right)^{1/2} \tag{22}$$

and an inflection point at

$$V_{\inf} = \left(-\frac{10c_{-4}}{3c_{-2}}\right)^{1/2} \tag{23}$$

If the potential energy coefficients c_{-4} and c_{-2} in Eq. (20) were temperature independent, plots of the internal energy versus volume at different temperatures would simply be identical curves shifted straight up or down depending on the temperature. This however is not the case. As temperature increases, the internal energy curve becomes more flat and the position of its minimum moves to the right.[16] This behavior is indicative of the fact that the coefficients c_{-4} and c_{-2} are temperature dependent. Furthermore, because $V_{\min}$ increases with temperature therefore, according to Eq. (22),

$$\frac{d}{dT}\left(-\frac{c_{-4}}{c_{-2}}\right) > 0 \tag{24}$$

Then according to Eq. (23),

$$\frac{dV_{\inf}}{dT} > 0 \tag{25}$$

But $V_{\inf}$ is the volume at which the internal pressure is a maximum.

The second interesting feature is that for a simple thermodynamic system we have

$$\left(\frac{\partial P}{\partial T}\right)_V = -\left(\frac{\partial V}{\partial T}\right)_P \Big/ \left(\frac{\partial V}{\partial P}\right)_T = \frac{\alpha}{\kappa_T} \tag{26}$$

where α is the coefficient of thermal expansion and κ_T is the isothermal compressibility.[17] The isothermal compressibility of any system is always positive.[18] The coefficient of thermal expansion is positive for most single-phase materials (including argon) with a few exceptions such as water between 0 °C and 3.98 °C and galium phosphide (GaP) below about 50 K.[19] Consequently, at constant volume the pressure of most systems (including argon) increases with temperature. The internal pressure of argon, however, *decreases* with temperature at constant volume.[16] This behavior, which was also verified in our molecular dynamics simulations, has been reported for a number of compounds as well.[13]

To give an account for a decrease of internal pressure with temperature at constant volume, we reiterate the fact that as the temperature increases the internal energy curve becomes more flat.[16] Therefore, the slope of the U–V curve decreases with temperature at constant volume, thus

$$\left(\frac{\partial}{\partial T}\right)_V \left(\frac{\partial U}{\partial V}\right)_T < 0 \tag{27}$$

which is equivalent to

$$\left(\frac{\partial P_{\text{int}}}{\partial T}\right)_V < 0 \tag{28}$$

Finally Goharshadi et al. have reported that all the properties described in this section for argon are shared by krypton and xenon, both experimentally and through molecular dynamics simulations.

3.2. Small/Nanosystems

As stated earlier, the main goal of this investigation is to study the functional dependence of the internal energy and internal pressure on volume in dense inert-gas nanosystems and to compare them with macroscopic systems. Some of the well-known characteristics of large systems are modified in small systems, and some of the relationships among various thermodynamic parameters in the former systems are changed in the latter ones. Thus, an investigation of this nature is essential for better understanding the thermodynamics of small systems.

In this part of our investigation, we used molecular dynamics again to simulate a generic three-dimensional system containing 8, 125, 512, and 1000 particles, interacting pairwise according to the Lennard-Jones potential energy function. The simulations were carried out on a Pentium III platform in Fortran 77 environment using the velocity form of the Verlet algorithm.[7, 20] We did not use periodic boundary conditions as in a small system surface atoms play a key role in determining its thermodynamic properties. For example, in a system containing 1000 atoms, roughly 500 atoms are immediately adjacent to the walls. And if the first two layers are excluded, a mere 216 atoms remain.[21] Using periodic boundary conditions will wash out surface effects and the simulation will not capture the state of the surface atoms. Thus, instead we allowed the particles to reflect elastically from the walls.

To avoid using very large or very small numbers, the computations were carried out using the following reduced system of units:[7, 22] mass of the particles m is the unit of mass, the hard-core radius of the Lennard-Jones potential σ is the unit of length, and the depth of the potential ϵ is the unit of energy. Thus, units of mass, length, and energy are respectively 6.63×10^{-26} kg, 3.40×10^{-10} m, and 1.67×10^{-21} J. It is then straightforward to show that in this system, the units of time, speed, and pressure are $\sigma(m/\epsilon)^{1/2} = 2.14 \times 10^{-12}$ s, $(\epsilon/m)^{1/2} = 159$ m/s, and $\epsilon/\sigma^3 = 4.25 \times 10^7$ Pa $= 419$ atm, respectively.

The unit of temperature, τ, is defined by

$$\tau = \frac{\epsilon}{k} = \frac{1.67 \times 10^{-21}\ \text{J}}{1.381 \times 10^{-23}\ \text{J/K}} = 121\ \text{K} \tag{29}$$

Thus, in this system of units, the Boltzmann constant has a value of one.

Since the temperature of the system is related to the particle speeds by[21]

$$T = \frac{1}{3N}\sum_{i=1}^{N} v_i^2 \tag{30}$$

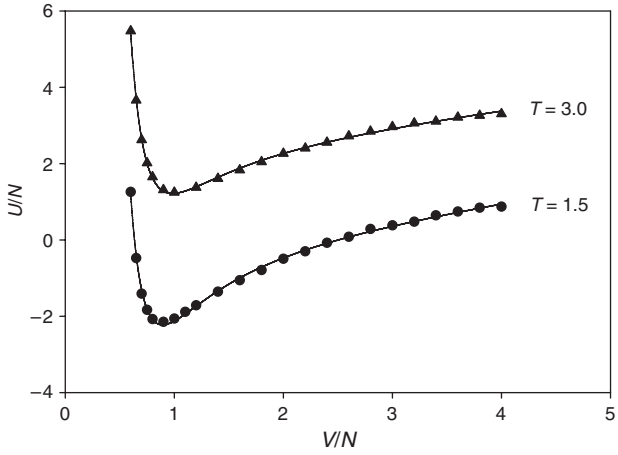

Fig. 3. Molecular dynamics data for the internal energy of 1000 argon-like particles as a function of volume at two different temperatures. The solid lines are the least-squares fits of the data to Eq. (33).

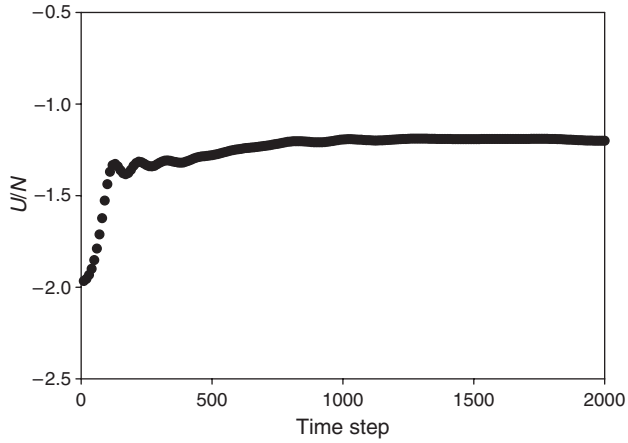

Fig. 5. Evolution of internal energy during the simulation of 1000 argon-like particles at $T = 1.5$ and $V/N = 1.5$, both in reduced units.

we maintained the temperature of the system by rescaling the velocity components after each time step according to[23, 24]

$$v_{ix}^{\text{new}} = v_{ix}\sqrt{\frac{T_D}{T_A}} \tag{31}$$

with similar expressions for the y and z components of the velocities, where T_A is the actual temperature of the system and T_D is the desired temperature.

The particles were initially placed on the points of a simple cubic lattice and were given an initial velocity of ± 0.1 reduced units along each coordinate direction, keeping the center of mass at rest. The velocities were then rescaled to the desired temperature. All simulations were carried out using a time step of 0.001 reduced unit.

Figure 3 shows the internal energy of a system of 1000 particles as a function of volume at two different temperatures, $T = 1.5$ and 3.0 reduced units. The simulation was carried out over 2000 time steps after thermalizing the system for 500 time steps. In order to ensure equilibrium and proper sampling during the simulation, we also collected data on the speed distribution function and the evolution of the internal energy per particle for a volume of 1.5 reduced unit. These results are shown in Figures 4 and 5. Figure 4 also shows the corresponding normalized Maxwell distribution function

$$f(v) = 4\pi\left(\frac{m}{2\pi kT}\right)^{3/2} v^2 \exp\left(-\frac{mv^2}{2kT}\right) \tag{32}$$

for $T = 1.5$, which is in excellent agreement with the simulation data.

When we tried to fit a function of the form given in Eq. (20) to the simulation data for 1000 particles, the result was very poor. However, with a linear term added,

$$U = c_{-4}V^{-4} + c_{-2}V^{-2} + c_0 + c_1 V \tag{33}$$

we obtained excellent fits at both temperatures, as shown in Figure 3. Again, the reason for this effect will be addressed in the next section. The constants in this equation corresponding to the best fits are given by

$$T = 1.5: \begin{bmatrix} c_{-4} = 1.41833 \\ c_{-2} = -3.40439 \\ c_0 = -0.570684 \\ c_1 = 0.430109 \end{bmatrix}$$

$$T = 3.0: \begin{bmatrix} c_{-4} = 1.33652 \\ c_{-2} = -2.59193 \\ c_0 = 2.12685 \\ c_1 = 0.352245 \end{bmatrix} \tag{34}$$

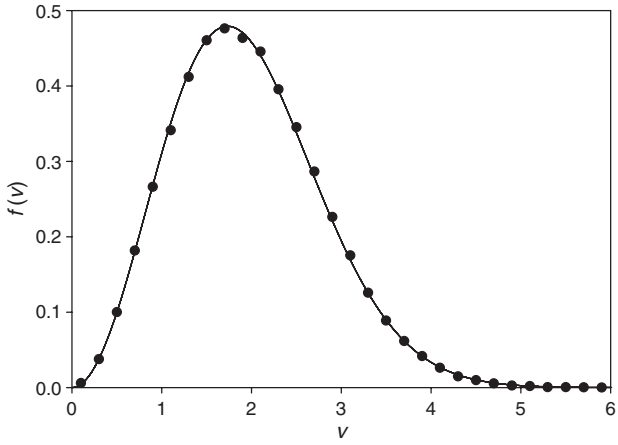

Fig. 4. Distribution of the atomic speeds for a system of 1000 argon-like particles at $T = 1.5$ and $V/N = 1.5$, both in reduced units. The solid line is the Maxwell distribution function at $T = 1.5$.

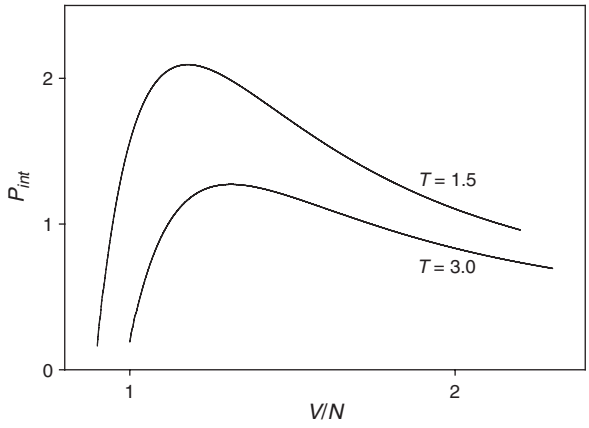

Fig. 6. Internal pressure for a system of 1000 argon-like particles as a function of volume at two different temperatures. The plots are calculated from the best fit of Eq. (33) to internal energy data in Figure 3.

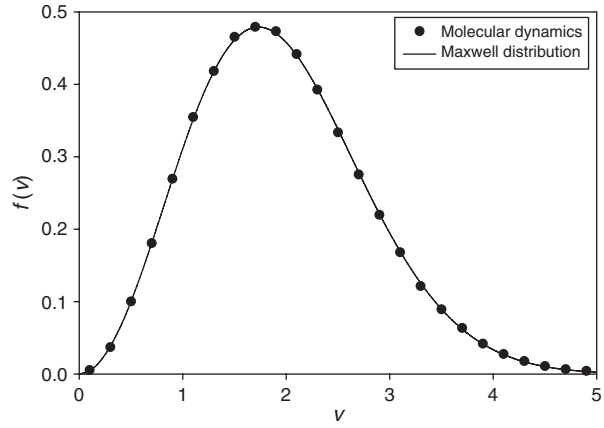

Fig. 8. Distribution of the atomic speeds for a system of 8 argon-like particles at $T = 1.5$ and $V/N = 1.5$, both in reduced units. The solid line is the Maxwell distribution function at $T = 1.5$.

where all quantities are in reduced units. Figure 6 shows the corresponding plots of the internal pressure as a function of volume derived from these best fits.

Figure 7 shows the molecular dynamics results of internal energy as a function of volume for a system of 8 particles at two different temperatures. Because sampling of a small system require longer simulation time to capture the states of the system, each data point was obtained over 2×10^6 time steps. Again in order to ensure equilibrium in the system, we have plotted the speed distribution function and the evolution of the internal energy during one of the runs at $T = 1.5$ and $V = 1.5$ reduced units in Figures 8 and 9. In Figure 8 we have also plotted the Maxwell distribution function at $T = 1.5$ for comparison.

Least-squares fits of the function in Eq. (33) to the simulation data for 8 particles produced very poor results at both temperatures. The fits obtained form Eq. (20) were even much worse. However, when a quadratic term was added to Eq. (33),

$$U = c_{-4}V^{-4} + c_{-2}V^{-2} + c_0 + c_1 V + c_2 V^2 \qquad (35)$$

the least-squares fits produced excellent results, which are shown by the continuous curves in Figure 7. The coefficients of Eq. (35) corresponding to these best fits are

$$T = 1.5: \begin{bmatrix} c_{-4} = 4.63086 \times 10^{-4} \\ c_{-2} = 1.26982 \times 10^{-2} \\ c_0 = 0.653585 \\ c_1 = 0.377119 \\ c_2 = -3.80306 \times 10^{-2} \end{bmatrix}$$

$$T = 3.0: \begin{bmatrix} c_{-4} = 4.21221 \times 10^{-4} \\ c_{-2} = 3.31646 \times 10^{-2} \\ c_0 = 3.33449 \\ c_1 = 0.230846 \\ c_2 = -1.74231 \times 10^{-2} \end{bmatrix} \qquad (36)$$

Figure 10 shows the internal pressures as a function of volume for the system of 8 particles derived from the above best fits to the internal energy at $T = 1.5$ and $T = 3.0$ reduced units.

Finally, we point out that the behaviors of the system consisting of 512 argon-like particles were similar to those consisting of 1000 particles with Eq. (33) giving the best fit to the U–V data, while those of 125-particle system

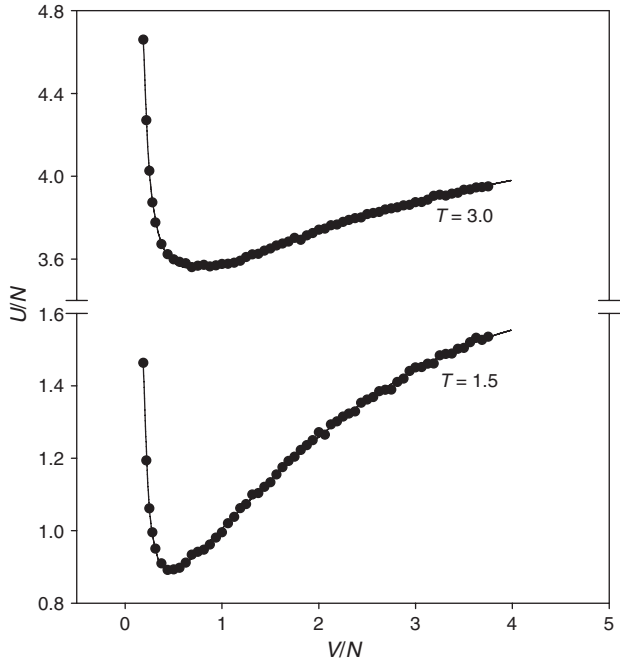

Fig. 7. Molecular dynamics data for the internal energy of 8 argon-like particles as a function of volume at two different temperatures. The solid lines are the least-squares fits of the data to Eq. (35).

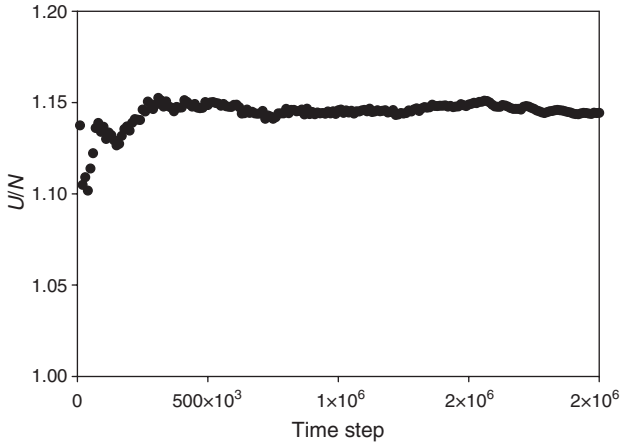

Fig. 9. Evolution of internal energy during the simulation of 8 argon-like particles at $T = 1.5$ and $V/N = 1.5$, both in reduced units.

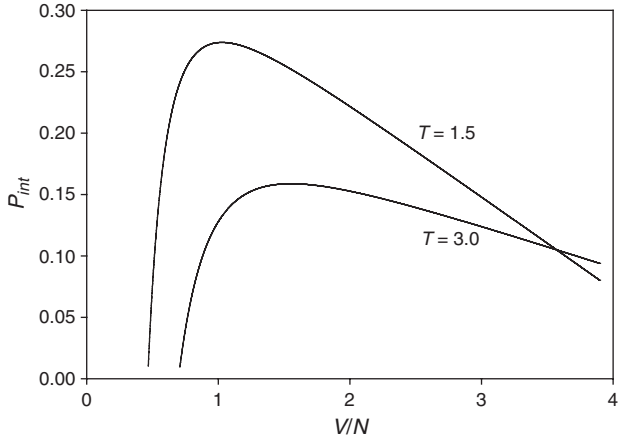

Fig. 10. Internal pressure for a system of 8 argon-like particles as a function of volume at two different temperatures. The plots are calculated from the best fit of Eq. (35) to internal energy data in Figure 7.

were similar to the 8-particle system with Eq. (35) giving the best fit to the U–V data.

4. DISCUSSION AND CONCLUSION

Early on in this article and along with other investigators we made two assumptions. First, that the volume of a closed thermodynamic system is proportional to the third power of mean nearest-neighbor distance between its particles. The second assumption was that the structure sums defined by Eq. (6) did not depend on the volume of the system. This assumption simply states that the geometry of the mean spacial configuration of the particles does not change with volume. Under these assumptions the equation for the internal energy of the system reduces to Eq. (20), in which c_0 is the kinetic energy term.

The validity of these assumptions depends on the success of Eq. (20) in explaining the experimental and simulational data. When we examined this equation against the experimental for argon, as well as the molecular dynamics data for 5000 argon atoms which mimic a macroscopic system, we discovered that the functional form of the equation was correct but the constant c_0 did not correctly represent the temperature of the system.

As the size of the system was reduced and periodic boundary conditions were removed, the functional form of internal energy versus volume at constant temperature began to change. With 1000 and 512 particles, a linear term in V was needed in Eq. (20) to properly represent the correct functional form of the U–V isotherm. When the size of the system was reduced further, even the addition of the linear term proved to be inadequate. With 125 and 8 particles, in addition to the linear term a quadratic term was needed.

These results are indicative of the fact that the two assumptions made earlier in this article, although reasonable in large systems, are not valid in small systems and hence the functional form of Eq. (20) does not correctly represent the U–V isotherm in these systems.

Let the correct function that describes the U–V isotherm of a system be $U_c = U_c(V)$. We denote the difference between this function and the function given in Eq. (20) by $f(V)$. Therefore,

$$U_c = c_{-4}V^{-4} + c_{-2}V^{-2} + c_0 + f(V) \tag{37}$$

For a system in which the two above mentioned assumptions are exactly satisfied, $f(V) = 0$. If on the other hand, the assumptions are only approximately valid, then the difference function $f(V)$ is not zero. Nevertheless, we can expand $f(V)$ in a power series about $V = 0$,

$$f(V) = a_0 + a_1V + a_2V^2 + \cdots \tag{38}$$

where the coefficients a_n are constants of the volume but may depend on the temperature.

For large systems, the only difference between the experimental data and Eq. (20) is in the constant term. This suggests that only the first term in the expansion of $f(V)$ is needed to bring Eq. (20) in line with the observed values. As the system becomes smaller, the difference between the observed values and Eq. (20) increases, thus requiring the second, and eventually the third term in the expansion of $f(V)$.

The results of this investigation indicate that the assumptions leading to Eq. (8) are, to a good approximation, valid for large systems but become less and less accurate as the size of the system decreases. These effects are in part attributed to the fact that for large systems the mean nearest-neighbor distance is a well-defined physical quantity. However, as the size of the system decreases with fewer and fewer number of particles in it, the mean nearest-neighbor distance becomes less and less well-defined. Consequently, Eq. (20), which is based on the validity of Eq. (8), ceases to approximate the correct functional form of the U–V isotherm.

A point that warrants clarification is that the replacement of microscopic variables in Eq. (2) with average values in the subsequent equations leading to Eq. (7) is an approximation, especially for small systems where fluctuations are important. Because in a canonical ensemble energy fluctuations are of the order of $N^{-1/225}$, these fluctuations can be large and introduce large errors. However, evolution of the energy of the system, both for 1000 particles as well as 8 particles, did not show unusually large fluctuations during the simulations, as can be seen in Figures 5 and 9. This is further supported by the near-Maxwellian distribution of the particle speeds in both cases as shown in Figures 4 and 8.

In conclusion, the assumptions of proportionality between the volume of a system and mean nearest-neighbor distance between its particles, a reasonable approximation in large systems, fail in small and nanosystems. Nevertheless, the qualitative behaviors, such as the volume dependence of the internal energy and internal pressure as well as the effect of temperature on them, are shared between large and small systems.

Acknowledgment: We would like to thank Dr. Elaheh K. Goharshadi for providing the experimental data as well as their molecular dynamics simulation data for 5000 argon particles.

References

1. T. L. Hill, Thermodynamics of Small Small Systems, Benjamin, New York **(1963)**, Vol. I.
2. T. L. Hill, Thermodynamics of Small Small Systems, Benjamin, New York **(1964)**, Vol. II.
3. T. L. Hill, *Nano Lett.* 1, 273 **(2001)**.
4. T. L. Hill, *Nano Lett.* 1, 111 **(2001)**.
5. T. L. Hill, *Nano Lett.* 1, 159 **(2001)**.
6. G. A. Mansoori, Principles of Nanotechnology, World Scientific, New Jersey **(2005)**.
7. P. Mohazzabi and G. A. Mansoori, *J. Comput. Theor. Nanosci.* 2, 138 **(2005)**.
8. K. Esfarjani and G. A. Mansoori, Handbook of Theoretical and Computatioanl Nanoscience and Nanotechnology **(2005)**, forthcoming.
9. J. M. Haile and G. A. Mansoori (eds.), Molecular-Based Study of Fluids, Avd. Chem. Series, 204, ACS, Washington D.C. **(1983)**.
10. E. Matteoli and G. A. Mansoori (eds.), Fluctuation Theory of Mixtures, Taylor & Francis, London **(1990)**.
11. D. A. McQuarrie, Statistical Mechanics, University Science Books, Herndon, VA **(2000)**.
12. R. K. Pathria, Statistical Mechanics, Pergamon, Oxford **(1993)**, p. 73.
13. A. F. M. Barton, *J. Chem. Ed.* 48, 156 **(1971)**.
14. H. B. Callen, Thermodynamics and an Introduction to Thermostatistics, 2nd edn., Wiley, New York **(1985)**, p. 182.
15. G. H. Wannier, Statistical Physics, Dover, New York **(1966)**, p. 136.
16. E. K. Goharshadi, A. Morsali, and G. A. Mansoori, *Chem. Phys.* 331, 332 **(2007)**.
17. H. B. Callen, Thermodynamics and an Introduction to Thermostatistics, 2nd edn., Wiley, New York **(1985)**, p. 84.
18. R. G. Mortimer, Physical Chemistry, 2nd edn., Academic Press, New York **(2000)**, p. 25.
19. K. Haruna, H. Maeta, K. Ohashi, and T. Koike, *J. Phys. C: Solid State Phys.* 19, 5149 **(1986)**.
20. H. Gould and J. Tobochnik, An Introduction to Computer Simulation Methods, 2nd edn., Addison Wesley, New York **(1996)**, pp. 123, 223–224.
21. D. C. Rapaport, The Art of Molecular Dynamics Simulation, Cambridge, Cambridge **(1995)**, p. 16.
22. H. Gould and J. Tobochnik, An Introduction to Computer Simulation Methods, 2nd edn., Addison Wesley, New York **(1996)**, p. 219.
23. J. M. Haile, Molecular Dynamics Simulation, Wiley, New York **(1992)**, p. 200.
24. G. A. Mansoori, Principles of Nanotechnology, World Scientific, New Jersey **(2005)**, pp. 157–158.
25. R. K. Pathria, Statistical Mechanics, Pergamon Press, New York **(1972)**, p. 70.

Received: 6 June 2007. Accepted: 14 June 2007.